Development 127, 1671-1679 (2000)
Printed in Great Britain © The Company of Biologists Limited 2000
DEV4301

Fate of the mammalian cranial neural crest during tooth and mandibular morphogenesis

Yang Chai[1,*], Xiaobing Jiang[2,5], Yoshihiro Ito[1], Pablo Bringas, Jr[1], Jun Han[1], David H. Rowitch[3], Philippe Soriano[4], Andrew P. McMahon[3] and Henry M. Sucov[5]

[1]Center for Craniofacial Molecular Biology School of Dentistry University of Southern California, 2250 Alcazar Street, CSA 103, Los Angeles, CA 90033, USA
[2]Program in Molecular Biology Department of Biological Sciences University of Southern California, 835 W. 37th Street, SHS 172, Los Angeles, CA 90089, USA
[3]Department of Molecular and Cellular Biology, Harvard University, 16 Divinity Avenue, Room 131, Cambridge, MA 02138, USA
[4]Division of Basic Sciences, Fred Hutchinson Cancer Research Center, 1100 Fairview Avenue North, PO Box 19024, Seattle, WA 98109, USA
[5]Institute for Genetic Medicine Keck School of Medicine University of Southern California, 2250 Alcazar Street, IGM 240, Los Angeles, CA 90033, USA
*Author for correspondence (e-mail: ychai@hsc.usc.edu)

Accepted 26 January; published on WWW 21 March 2000

SUMMARY

Neural crest cells are multipotential stem cells that contribute extensively to vertebrate development and give rise to various cell and tissue types. Determination of the fate of mammalian neural crest has been inhibited by the lack of appropriate markers. Here, we make use of a two-component genetic system for indelibly marking the progeny of the cranial neural crest during tooth and mandible development. In the first mouse line, Cre recombinase is expressed under the control of the *Wnt1* promoter as a transgene. Significantly, *Wnt1* transgene expression is limited to the migrating neural crest cells that are derived from the dorsal CNS. The second mouse line, the ROSA26 conditional reporter (*R26R*), serves as a substrate for the Cre-mediated recombination. Using this two-component genetic system, we have systematically followed the migration and differentiation of the cranial neural crest (CNC) cells from E9.5 to 6 weeks after birth. Our results demonstrate, for the first time, that CNC cells contribute to the formation of condensed dental mesenchyme, dental papilla, odontoblasts, dentine matrix, pulp, cementum, periodontal ligaments, chondrocytes in Meckel's cartilage, mandible, the articulating disc of temporomandibular joint and branchial arch nerve ganglia. More importantly, there is a dynamic distribution of CNC- and non-CNC-derived cells during tooth and mandibular morphogenesis. These results are a first step towards a comprehensive understanding of neural crest cell migration and differentiation during mammalian craniofacial development. Furthermore, this transgenic model also provides a new tool for cell lineage analysis and genetic manipulation of neural-crest-derived components in normal and abnormal embryogenesis.

Key words: Cre recombinase, *lacZ*, Mammalian neural crest, Mandible formation, ROSA26 conditional reporter (R26R), Tooth formation, Transgenic mice, *Wnt1* promoter

INTRODUCTION

The vertebrate neural crest is a pluripotent cell population derived from the lateral ridges of the neural plate during early stages of embryogenesis. Neural crest cells disperse from the dorsal surface of the neural tube and migrate extensively through the embryo, giving rise to a wide variety of differentiated cell types (Romer, 1972; Noden, 1983; Tan and Morriss-Kay, 1986; Bronner-Fraser, 1993). Considerable progress has been made in recent years towards understanding how this important population of pluripotent cells is initially established in the early embryo, and how genetic and epigenetic mechanisms mediate their subsequent lineage segregation, differentiation and final contribution to a particular cell type (see review by LaBonne and Bronner-Fraser, 1999).

During craniofacial development, neural crest cells migrate ventrolaterally as they populate the branchial arches. The proliferative activity of these crest cells produces the discrete swellings that demarcate each branchial arch. As these ectodermally derived cells migrate, they contribute extensively to the formation of mesenchymal structures in the head and neck. Cell labeling studies have demonstrated that neuroectoderm cells of rhombomeres 1-4 (r1-4) in the forming posterior midbrain and anterior hindbrain transform into CNC cells, which migrate into the first branchial arch and thereafter reside within the maxillary and mandibular prominences (Osumi-Yamashita et al., 1990; Serbedzija et al., 1992;

Bronner-Fraser, 1993; Selleck et al., 1993; Lumsden and Krumlauf, 1996). The migration of these rhombencephalic crest cells may be regulated by growth factor signaling pathways and their downstream transcription factors before they become committed to a number of different cell types including progenitor tooth mesenchymal cells, osteoblasts, chondroblasts and cranial nerve ganglia of the branchial arch (Noden, 1983, 1991; Lumsden, 1988; Graham and Lumsden, 1993; Le Douarin et al., 1993; Echelard et al., 1994; Imai et al., 1996). Studies using chick-quail chimeras (Noden, 1983), cell labeling with a vital dye such as DiI (Serbedzija et al., 1989, 1992), neural-crest-cell-specific antibodies (Tucker et al., 1984) and retroviral-mediated gene transfer (Poelmann and Gittenberger-de Groot, 1999) have significantly advanced our understanding of migration and differentiation pathways of these multipotent stem cells during embryogenesis. However, a comprehensive cell lineage analysis of the mammalian neural crest cells as they become terminally differentiated to become a particular cell type has been limited by the lack of a genetic marker that would allow these cells to be followed indefinitely.

The proto-oncogene *Wnt1* encodes a short-range signal and is only expressed during development of the central nervous system (Wilkinson et al., 1987; McMahon et al., 1992; Echelard et al., 1994). *Wnt1* expression is initiated at neural plate stages throughout the presumptive midbrain, then becomes rapidly restricted to a tight circle lying just anterior of the midbrain/hindbrain isthmus by neural tube closure. Spontaneous and targeted mutation of *Wnt1* resulted in the loss of the midbrain and led to a secondary loss of anterior hindbrain (Thomas et al., 1991; Thomas and Capecchi, 1990; McMahon and Bradley, 1990; McMahon et al., 1992). Interestingly, the first crest cells arise in the midbrain/hindbrain regions at the 4-somite stage in the mouse and emigration is completed by 7- to 14-somite stage (Nichols, 1981; Chan and Tam, 1988; Serbedzija et al., 1992). Significantly, cranial and spinal ganglia, and skeletogenic neural crest cells in the branchial arches are all derived from *Wnt1*-expressing precursor cells in CNS. Transgenic lines expressing β-galactosidase under the control of *Wnt1* promoter demonstrate staining in the CNS, identical to the expression pattern of the endogenous *Wnt1* gene, and show staining in the population of neural crest initially emigrating away from the neural tube (Echelard et al., 1994). Thus, *Wnt1-lacZ* transgene expression provides a new tool for analysis of neural crest development.

In order to use *Wnt1-lacZ* expression as a marker to follow the migration and differentiation of neural crest cells, the transgene has to be active throughout embryogenesis and beyond. However, with this *Wnt1-lacZ* transgene, β-galactosidase-positive cells are not seen in later embryos, accurately reflecting the cessation of *Wnt1* gene expression in the neural crest progeny and preventing its use for following the differentiation of neural crest cells. To solve this problem, we use the Cre/lox system. The *Wnt1-Cre* transgene mediated DNA recombination after being crossed with the ROSA26 conditional reporter (*R26R*) transgene. *R26R* exhibits constitutive β-gal expression in all cells when activated by ubiquitously expressed Cre, and is ideal for monitoring Cre-mediated expression and cell lineage analysis in both developmental and postnatal times (Soriano, 1999). By utilizing the *Wnt1* promoter, Cre expression was restricted to the precursors of the neural crest. Consequently, the progeny of the neural crest is marked indelibly during embryogenesis. Using this two-component genetic system, we have systematically followed the dynamic contribution of CNC cells during tooth and mandibular morphogenesis. More importantly, this transgenic approach allows the analysis of the fate and function of mammalian neural crest to be integrated with mouse molecular genetics in both normal and abnormal embryonic development.

MATERIALS AND METHODS

Animals and tissue preparation

Both the *Wnt1-Cre* transgenic line and the *R26R* conditional reporter allele have been described previously (Danielian et al., 1998; Soriano, 1999). The animals were maintained on a light-dark cycle with light from 0600 to 1800 hours. Mating *Wnt1-Cre*$^{+/-}$ with *R26R*$^{+/-}$ mice generated *wnt1-Cre/R26R* mice (double transgenic). Embryonic age was determined according to the vaginal plug, with noon of the day of plug observation as E0.5. External staging was used to define embryonic development according to the number of somite pairs (Theiler, 1989).

Genotypes of the double transgenic embryos and adult animals were determined by PCR. Genomic DNA was isolated from yolk sac and tail biopsies of live embryos, fetuses, newborns and adults. The 5′ and 3′ primers used for detecting *Wnt1-Cre* gene were primer 1 (5′-ATTCTCCCACCGTCAGTACG-3′) and primer 2 (5′-CGTTTTC-TGAGCATACCTGGA-3′). Three oligonucleotides were used to genotype *R26R* transgenic animals as previously reported (Soriano, 1999).

Detection of β-galactosidase (*lacZ*) activities

Whole embryos (E9.5 and E10.5) were stained for β-galactosidase activity according to the standard procedures. Embryos were fixed for 20 minutes at room temperature in 0.2% glutaraldehyde in phosphate-buffered saline (PBS). Fixed embryos were washed three times in rinse solution (0.005% Nonidet P-40 and 0.01% sodium deoxycholate in PBS). Embryos were stained overnight at room temperature using the standard staining solution (5 mM potassium ferricyanide, 5 mM potassium ferrocyanide, 2 mM $MgCl_2$, 0.4% X-gal in PBS), rinsed twice in PBS and postfixed in 3.7% formaldehyde. Both E9.5 and E10.5 embryos were sectioned to observe *lacZ* expression at the cellular level. The embryos were dehydrated through alcohol and embedded in paraffin. Sections were cut at 10 μm thickness and counterstained with Nuclear Fast Red.

Cryostat sectioning

E11.5 to newborn mouse tissue was frozen sectioned and stained according to the standard procedure as follows. Tissue was dissected in PBS, fixed by immersion in 0.2% glutaraldehyde solution for 30 minutes at room temperature, soaked in 10% sucrose in PBS for 30 minutes at 4°C, incubated in PBS plus 2 mM $MgCl_2$, 30% sucrose and 50% OCT at 4°C for 2 hours, frozen in OCT and chilled on dry ice. Sections were cut at 20 μm thickness, mounted on gelatin-coated slides, fixed in 0.2% glutaraldehyde for 10 minutes on ice, and rinsed briefly in PBS with 2 mM $MgCl_2$, followed by a 10 minute wash in the same solution on ice. The tissue sections were incubated in detergent rinse solution (0.005% NP-40 and 0.01% sodium deoxycholate in PBS) for 10 minutes at 4°C, stained in X-gal staining solution overnight at room temperature in the dark and counterstained with Nuclear Fast Red and Eosin. Adult transgenic mouse heads (6 weeks old) were dissected free of the soft tissue, frozen on dry-ice for 1 hour, sectioned at 200-400 μm thickness using a diamond disk with a slow-speed dental handpiece and stained following the whole-mount staining procedures.

Scanning electron microscopy

Embryonic specimens were processed and viewed according to standard procedure (Chai et al., 1997).

RESULTS

Contribution of CNC cells during early craniofacial development

By crossing Wnt1-Cre with R26R mice, we have generated transgenic animals expressing β-galactosidase in migrating neural crest cells. Once *Wnt1-Cre* expression commences in premigrating neural crest cells, the β-galactosidase is indelible, allowing us to analyze neural crest cell lineage. At E9.5 in mouse development (21-29 somites, Theiler stage 15), the anterior neuropore is closed (Fig. 1A), and the frontonasal prominence, first and second branchial arches are clearly visible. In *Wnt1-Cre*/*R26R* transgenic mice, the *lacZ* expression pattern is co-localized with the expected distribution pattern of CNC cells, including the frontonasal prominence, first and second branchial arches and spinal dorsal root ganglia (Fig. 1B). At a higher magnification, CNC-derived cells are clearly visible in frontonasal prominence, the first arch, trigeminal ganglia (with V1, ophthalmic division visible), second arch and facial nerve ganglia (Fig. 1C).

At E10.5 (35-39 somites, Theiler stage 17), the first branchial arch has divided into maxillary and mandibular prominences. The second arch is well formed (Fig. 1D). In *Wnt1-Cre*/*R26R* transgenic embryos, *lacZ* expression is prominent in frontonasal prominence surrounding the olfactory pit, both maxillary and mandibular prominences, trigeminal nerve ganglia, second arch along with facial nerve ganglia, glossopharyngeal nerve ganglia and primordium of the third branchial arch, and vagus nerve ganglia behind the future fourth branchial arch (Fig. 1E). At a higher magnification, the progeny of CNC cells are localized in area surrounding olfactory pit, maxillary and mandibular prominences along with the trigeminal nerve (with V1 clearly visible), the second branchial arch and facial nerve ganglia, and glossopharyngeal nerve ganglia (Fig. 1F).

When *Wnt1-Cre/R26R* embryos are serially sectioned, X-gal-positive CNC-derived cells are present throughout the craniofacial region (Fig. 2). At E9.5, CNC-derived cells densely populate both the first and second branchial arches (Fig. 2A). Non-CNC-derived mesenchymal cells, although in small numbers, are also present within the branchial arch intermingling with crest-derived cells. Significantly, the epithelium that covers each branchial arch does not show any *lacZ* expression (Fig. 2B). At E10.5, CNC cells from the posterior midbrain and rostral hindbrain region (Serbedzija et al., 1992) migrate ventrolaterally along a subectodermal pathway and populate the first branchial arch (Fig. 2C). When examined closely, CNC-derived cells populate the region immediately underneath the first arch ectoderm, although without any integration into the ectoderm (Fig. 2D). As embryogenesis continued, CNC cells further populate the first arch at E11.5. CNC-derived cells are closely associated with the ectoderm (Fig. 2F). Because the tissue was sectioned first and then stained for *lacZ* expression, the close association between CNC-derived cells and oral ectoderm was clearly not due to an incomplete penetration of the staining solution but a possible representation of the critical epithelial-mesenchymal interaction that regulates the subsequent formation of various structures in the branchial arch.

Contribution of CNC cells during tooth morphogenesis

Tooth formation requires a series of reciprocal epithelial-mesenchymal interactions. The initial inductive signal of tooth formation resides in oral epithelium and later in development shifts into the CNC-derived ectomesenchyme (Koch, 1967; Kollar and Baird, 1969; Kollar and Lumsden, 1979; Mina and Kollar, 1987; Lumsden, 1988; Thesleff and Sharpe, 1997; Tucker et al., 1998). Numerous growth and transcription factors belonging to several different families have been associated with epithelial-mesenchymal signaling during tooth morphogenesis (Thesleff and Sharpe, 1997). Here we demonstrate systematically, for the first time, that CNC-derived ectomesenchyme contributes to the formation of condensed dental mesenchyme at the initial budding stage of tooth formation and then to the formation of dental papilla mesenchyme, preodontoblast, odontoblast/dentin matrix, pulp, cementum and periodontal ligament.

At E12.5, CNC-derived ectomesenchyme is closely associated with the first arch ectoderm (Fig. 3A). Initiation of tooth morphogenesis starts at E12 with the formation of dental lamina. As shown in Fig. 3B, there is no *lacZ* expression in ectodermally derived dental lamina, while strong *lacZ* expression is present in CNC-derived ectomesenchyme surrounding the dental lamina. As tooth development continues into early bud stage at E13.5, condensed dental mesenchyme is mainly populated with CNC-derived cells (Fig. 3C). The enamel organ epithelium along with oral ectoderm remains free of *lacZ* expression. At E14.5 (late bud stage), a significant number of CNC-derived ectomesenchymal cells, along with some non-CNC cells, are present in condensed dental mesenchyme surrounding the enamel organ epithelium (Fig. 3D). As the tooth bud continues to proliferate, unequal growth in the different parts of the bud leads to formation of the cap stage, characterized by a shallow invagination on the deep surface of the bud (Fig. 3E,F) at E15.5. Outer and inner enamel epithelium, including enamel knot, are free of *lacZ* expression, accurately reflecting their ectodermal origin. The dental papilla, the mesenchyme partially enclosed by the invaginated portion of the inner enamel epithelium, and the dental sac, concomitant with the development of the enamel organ and dental papilla, are populated with CNC-derived cells as well as an increasing amount of non-CNC cells (Fig. 3F).

Because of variation in tooth development, it is not unusual to observe different stages of tooth organogenesis at a particular embryonic time point, e.g. the tooth organs in Fig. 3E,F are at an earlier stage than that in Fig. 4A. Nevertheless, CNC-derived ectomesenchyme is clearly present within dental papilla and dental sac, while both inner and outer enamel epithelium is free of *lacZ* expression (Fig. 4B). At E17.5, β-gal-positive cells mark the progeny of CNC-derived cells in the dental papilla of a molar tooth organ (Fig. 4C). Noticeably, non-CNC-derived cells are more prominent within dental papilla compared to the earlier stages of tooth development. At the boundary between the inner enamel epithelium and dental papilla, CNC-derived preodontoblasts are lined up to form

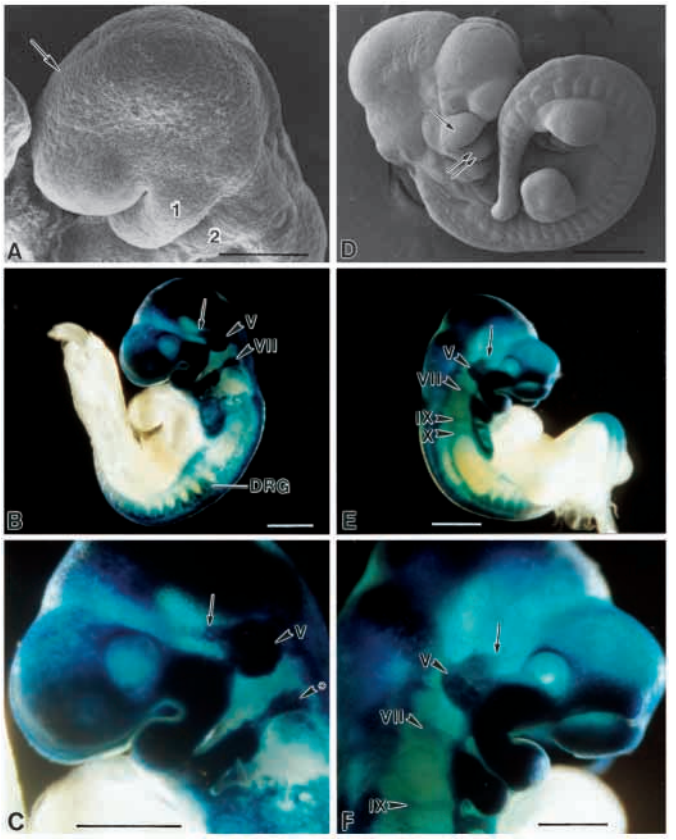

Fig. 1. Contribution of CNC cells during early craniofacial development. (A) Scanning electron microscope image of an E9.5 mouse embryo. The anterior neuropore is closed (arrow). The first and second branchial arches are present. (B) Whole-mount staining of E9.5 *Wnt1-Cre/R26R* embryo shows CNC-derived cells (dark blue) in the first and second branchial arches. Trigeminal ganglia (V) is present behind the first arch, with the ophthalmic division clearly visible (arrow). Facial nerve ganglia can be seen behind the second arch (VII). Strong β-gal staining is also present in dorsal root ganglia (DRG). (C) CNC-derived cells populate both the first and second arches with trigeminal (V) and facial nerve (*) ganglia, respectively. (D) Scanning electron microscope image of an E10.5 mouse embryo. The first arch has given rise to both maxillary (single arrow) and mandibular (double arrow) prominences. The most cranial somites are more indistinct. (E) The first, second and the rudimentary third arch all show CNC-derived cells in this whole-mount specimen. Trigeminal (V), facial (VII), glossopharyngeal (IX) and vagus (X) nerve ganglia are positive for *lacZ* expression, indicating CNC origin. (F) Population of CNC cells is present in frontonasal prominence, maxillary, mandibular prominences and the second arch. Single arrow, ophthalmic division of trigeminal nerve. Scale bars: A, 200 μm; B,C,F, 0.5 mm; D, 500 μm; E, 1 mm.

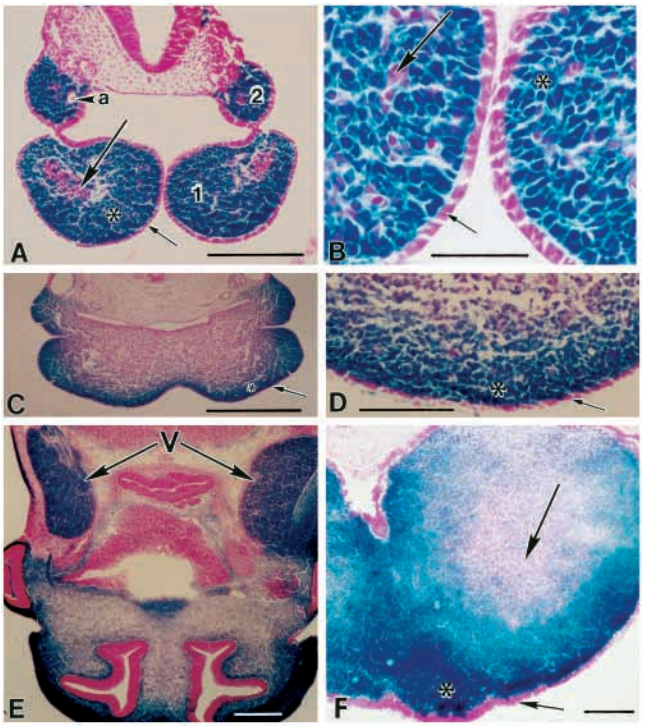

Fig. 2. Patterning of CNC cells in the branchial arches during early craniofacial development. (A) At E9.5, both the first and second branchial arches are almost entirely populated by CNC-derived cells (*). Non-CNC-derived cells (large arrow) are present in small number within the branchial arch. The epithelium is completely free of *lacZ* expression (small arrow). a, the second arch aorta. (B) CNC-derived ectomesenchyme is closely associated with epithelium, with few non-CNC-derived cells (large arrow) present. (C) At E10.5, CNC-derived cells are in close association with the primordial oral epithelium. (D) The oral epithelium clearly does not express *lacZ* (small arrow). CNC-derived cells (*) are in close contact with the epithelium. (E) At E12.5, a cross-section of cranial region shows trigeminal ganglia is mainly populated with CNC-derived cells (V). (F) A transverse-section of the E11.5 first branchial arch indicates that CNC-derived cells (*) are more concentrated under oral epithelium (small arrow). Large number of non-CNC-derived cells is present within middle of the arch (large arrow). Scale bars: A,C, 0.5 mm; B, 50 μm; D,F, 100 μm; E, 250 μm.

dentin matrix, while preameloblasts are free of any *lacZ* expression (Fig. 4D).

To identify the fates of CNC-derived ectomesenchymal cells, we obtained samples from 6-week-old *Wnt1-Cre/R26R* transgenic mice. In a cross-section of maxillary molars, odontoblasts, dentine matrix, pulp tissue, cementum and periodontal ligaments show strong *lacZ* expression, indicating their CNC origin. The enamel is free from any staining (Fig. 4E,F). Mandibular molars and incisors contain CNC-derived cells in the same tissues as in the maxillary molars. As expected, non-transgenic littermates do not express *lacZ* (Fig. 4G).

Rodent lower incisors continue to grow throughout their life span. At E17.5, lower incisors are present on both sides of Meckel's cartilage (Fig. 6E). CNC-derived *lacZ*-expressing odontoblasts are present on top of the dental papilla adjacent to the inner enamel epithelium. Noticeably elongated enamel epithelium (the proliferating zone) extends down towards the molar region in the mandible. The entire dental papilla under the enamel epithelium is populated with CNC-derived cells. In adulthood, part of lower incisor is present under the apical region of lower molar. The pulp and odontoblasts show strong *lacZ* expression, while the enamel is free of any staining (Fig. 6G).

In summary, our two-component transgenic system allows us to identify the contribution of CNC cells during tooth

morphogenesis. We are able to clearly follow the progeny of CNC-derived cells from initiation of tooth formation into differentiated tooth-related cell types in the adult (Fig. 5). These results confirmed that the transgene is expressed throughout the entire lineage of neural crest derivatives. The specificity of this transgenic system is demonstrated by the absence of any ectopic *lacZ* expression in non-CNC-derived tissue.

Contribution of CNC cells during mandibular morphogenesis

Craniofacial skeletogenesis and myogenesis occur within mesenchymal cell population. CNC-derived cells contribute to skeletogenesis in the regions formed by frontonasal and branchial arch prominences, while all voluntary craniofacial muscles derive from paraxial mesoderm in birds (Noden, 1983). In mammals, recent studies using various cell-labeling techniques have demonstrated that CNC cells migrate into frontonasal and branchial arch prominences. The migration and destination of crest cells are dependent of their axial level as well as their developmental stage at initial emigration

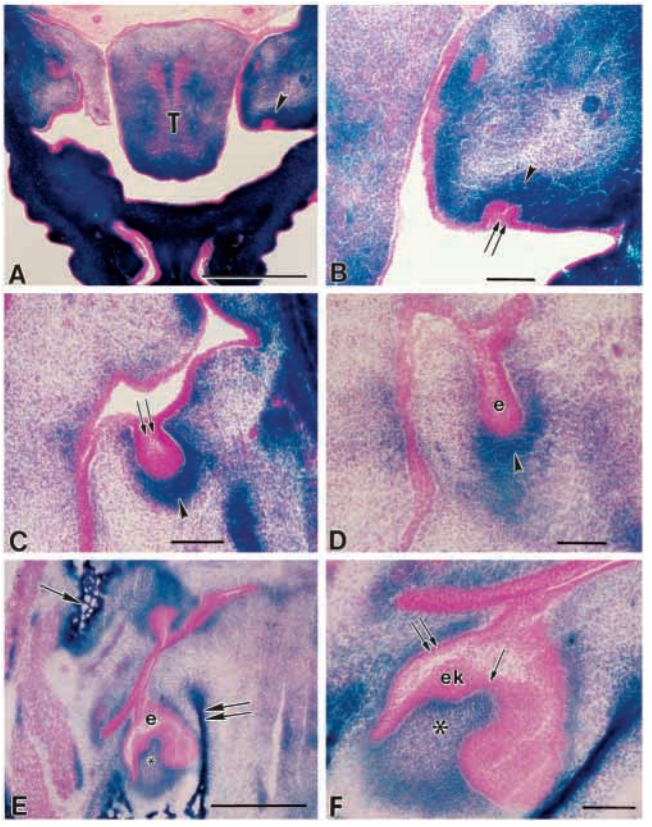

Fig. 3. The contribution of CNC-derived cells during tooth morphogenesis. (A) At E12.5, the initiation of tooth morphogenesis is marked by dental lamina formation. Condensed dental mesenchyme is heavily populated with CNC-derived cells (arrowhead). T, tongue. (B) The dental lamina does not express *lacZ* (double arrow). The entire dental mesenchyme is populated with CNC-derived cells (arrowhead). (C) At E13.5, tooth formation has advanced into early bud stage (double arrow). The condensed dental mesenchyme is largely populated with CNC-derived cells (arrowhead). (D) At E13.5, the elongated enamel epithelium (e) has developed into the late bud stage. Most of the condensed dental mesenchymal cells express *lacZ*, while some non-CNC-derived cells (pink) are also present surrounding the enamel epithelium. (E) At E15.5, a cap stage tooth organ is present with both CNC-derived (*) and non-CNC-derived cells within the dental papilla. Both mandible (double arrow) and maxilla (single arrow) contain β-gal-positive cells. (F) Enamel knot (ek), inner enamel epithelium (single arrow) and outer enamel epithelium (double arrow) do not contain β-gal-positive cells. The dental papilla is populated with both CNC-derived (*) and non-CNC-derived cells. Scale bars: A,E, 0.5 mm; B-D,F, 100 μm.

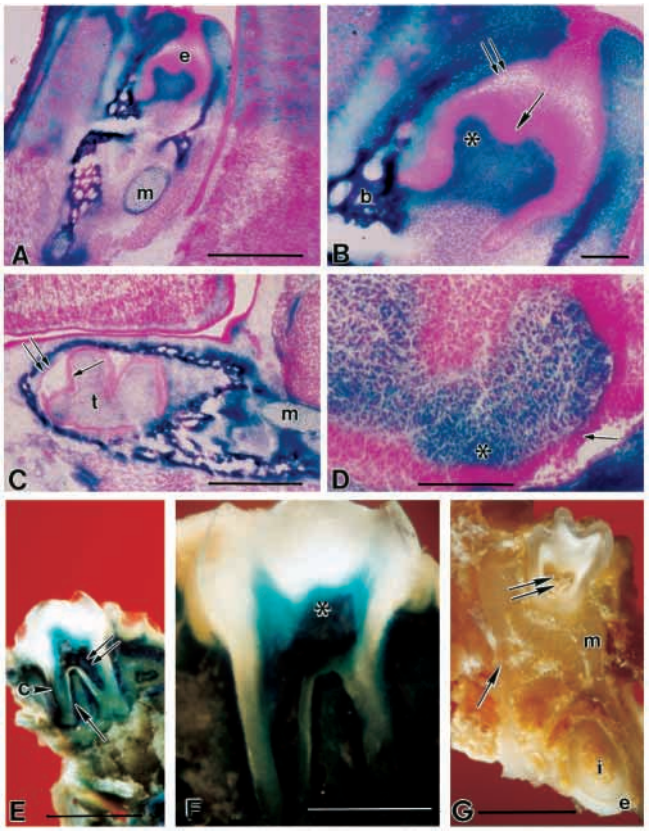

Fig. 4. The contribution of CNC-derived cells during tooth morphogenesis (continued). (A) There is variation in the stage of tooth morphogenesis at a given embryonic time point. Here at E15.5, tooth formation has advanced into bell stage with the folding of the enamel epithelium (e). The dental papilla and Meckel's cartilage (m) show large numbers of CNC-derived cells. (B) Both inner (single arrow) and outer (double arrow) enamel epithelium do not contain β-gal-positive cells. The dental papilla is populated with mainly CNC-derived cells (*), while some β-gal-negative cells are also present. b, mandible. (C) At E17.5, a tooth organ (t) is present within the mandible. Both inner (single arrow) and outer (double arrow) enamel epithelium is free of β-gal-positive cells. (D) The dental papilla is populated with both CNC- (*) and non-CNC-derived cells adjacent to preameloblasts (single arrow). (E) In a cross section of maxilla of a 6-week-old adult transgenic mouse, β-gal-positive cells are present in dentine, pulp (double arrow), cementum (c) and periodontal ligament (single arrow). (F) The adult maxillary molar is shown with β-gal-positive cells in dentine (*), pulp, cementum and periodontal ligament, reflecting their CNC origin. (G) An adult mouse non-transgenic littermate control does not show any labeling in mandible (m), pulp tissue of both incisors (i) and molars. Double arrow, molar pulp; single arrow, mandibular periosteum. Scale bars: A,C,F, 0.5 mm; B,D, 100 μm; E,G, 1 mm.

(Serbedzija et al., 1992; Osumi-Yamashita et al., 1994; Imai et al., 1996). There has never been a direct cell lineage analysis in mammals, however, demonstrating the contribution of CNC-derived cells to the formation of Meckel's cartilage, mandible and other craniofacial skeletal structures.

Meckel's cartilage begins to form as an aggregated cell mass in the future molar region within the mandibular arch and it extents both anteriorly and posteriorly to form a template for mandible formation (Chai et al., 1994, 1998). At E12.5, an aggregated cell mass containing CNC-derived cells is present within the mandible (Fig. 6A). These CNC-derived ectomesenchymal cells are responsible for the formation of Meckel's cartilage. As embryogenesis continues, CNC-derived cells are mixed with non-CNC-derived cells within Meckel's cartilage at E13.5 (Fig. 6B). Perichondrium is also β-gal-positive, indicating its CNC origin. CNC-derived ectomesenchyme continues to be present throughout the chondrogenesis of Meckel's cartilage at E14.5 and E15.5 (Fig. 6C,D). At E17.5, the anterior (rostral) region of Meckel's cartilage is formed with the presence of a larger number of CNC-derived cells than the posterior portion of the cartilage (Fig. 6E). A higher percentage of β-gal-positive cells are always associated with the chondrogenic front of Meckel's cartilage as it elongates both anteriorly and posteriorly within the mandibular arch. At birth, mandible is formed with a significant contribution of CNC-derived ectomesenchyme (Fig. 6F). 6 weeks after birth, the mandible and its periosteum (Fig. 6G), the palatine bone and its periosteum (Fig. 6H) and the articulating disc of temporomandibular joint (TMJ; Fig. 6I) are β-gal positive, indicating the contribution of CNC cells.

DISCUSSION

Our two-component genetic system has demonstrated a novel and effective method of indelibly marking the progeny of CNC cells during tooth and mandibular morphogenesis. The fidelity of the expression pattern that we have observed is a consequence of the exceptional expression specificity of the *Wnt1* promoter in neural crest cells, and the specifically activated *R26R* reporter gene expression (Echelard et al., 1994; Danielian et al., 1998; Zambrowicz et al., 1997; Soriano, 1999). Using this two-component genetic system, we have shown that CNC cells migrate into the branchial arch, interact with both ectoderm- and paraxial mesoderm-derived cells to form various structures during embryogenesis. CNC-derived ectomesenchymal cells first migrate into the branchial arch, populating the majority of arch mesenchyme (Fig. 2A), and later become more localized under the oral ectoderm to form various structures through critical epithelial-mesenchymal interactions (Figs 5, 6). Significantly, our study provides a much more detailed information on the precise location and the dynamic distribution pattern of these CNC-derived cells throughout embryogenesis.

Neural crest cells contribute significantly to the formation of craniofacial structures during embryonic development. These cells first migrate into the first branchial arch from the midbrain and anterior hindbrain around the 4-somite stage (Nichols, 1981; Tan and Morris-Kay, 1986; Serbedzija et al., 1992; Chai et al., 1998). Most of these studies, however, relied on dye labeling, tissue transplantation and viral transfection of neural crest cells. Because of the difficulties in culturing embryos, microsurgical manipulation of embryonic tissue and maintaining the dye throughout the long period of embryogenesis, it was not possible to obtain a systematic lineage analysis of neural crest cell derivatives in mammals. Moreover, there was no guarantee that all neural crest cells were labeled using either dye labeling or viral infection techniques. Recently, a transgenic approach similar to ours but using a conditional reporter gene driven by chick β-actin promoter and mediated by P0-Cre demonstrated the application of the two-component genetic system in marking neural crest cell derivatives (Yamauchi et al., 1999). However, the P0-Cre-mediated DNA recombination only revealed incomplete expression of the reporter gene in neural-crest-derived tissue with significant ectopic expression. This clearly indicates the importance of the highly regulated promoter components used in our *Wnt1-Cre/R26R* to achieve very specific neural crest cell labeling.

The biological function of these CNC-derived cells has been studied in a variety of animal models and two possible theories have been put forth. First, these neural crest cells may carry certain preacquired molecular signals as they migrate into the branchial arch so they can induce epithelium to form various craniofacial structures. Recent studies on zebrafish development have shown that CNC cells have acquired regional identity before making the initial contact with axial mesoderm and certain mutations can reduce the number of early neural crest cells and affect the formation of CNC-derived structures (Woo and Fraser, 1998; Artinger et al., 1999). More importantly, endogenous Wnt signaling within premigratory neural crest cells may contribute to the diversity of neural crest cell fates (Dorsky et al., 1998). Second, CNC cells acquire positional identity at the time they reach their final destination and contribute to the formation of various craniofacial structures. Certain growth and transcription factors have been implicated as important regulators for the critical epithelial-mesenchymal interactions through which these multipotent neural-crest-derived cells become progressively restricted to form neural crest derivatives and eventually develop into individual cell types (Bronner-Fraser, 1995; Sharpe, 1995; Thesleff and Sharpe, 1997; Anderson, 1997; Saldivar et al., 1997; Tucker and Sharpe, 1999). For example, targeted mutation of the *Wnt1* and *Wnt3a* genes results in a marked deficiency in neural crest derivatives (Ikeya et al., 1997). Mutation of the *Sox10* gene affects mouse neural-crest-derived cranial ganglia development (Herbarth et al., 1998). Selective FGF8 inactivation in surface ectoderm affected the outgrowth and patterning of the first branchial arch, indicating that FGF8 is critical for the survival of CNC-derived ectomesenchyme and can induce a developmental program required for the first branchial arch morphogenesis (Trumpp et al., 1999). Significantly, our two-component genetic system offers a new opportunity to test these theories by crossing our transgenic stocks with mice carrying particular mutations that affect tooth and mandibular morphogenesis.

CNC cells contribute significantly to tooth morphogenesis (Smith and Hall, 1993; Thesleff and Sharpe, 1997; Tucker and Sharpe, 1999). The initial indication of tooth formation is a thickening of the oral epithelium, which subsequently buds into the underlying mesenchyme. Through the critical and continued interactions between oral epithelium and CNC-

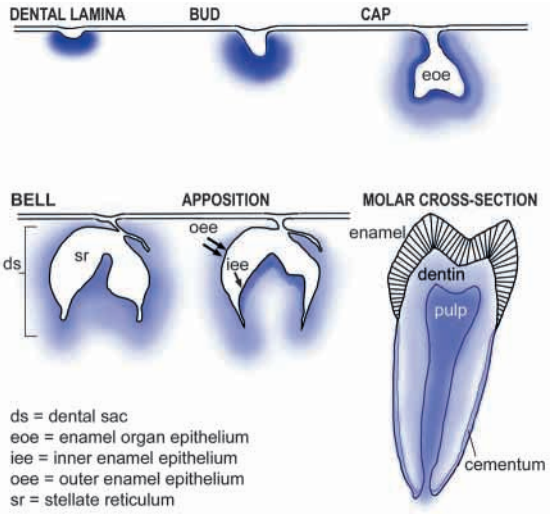

Fig. 5. Schematic drawing of life cycle of tooth with contribution from CNC cells. When tooth development is initiated with the formation of dental lamina, its underlying mesenchyme is almost entirely populated with CNC-derived cells (dark blue). As the tooth develops from bud to cap stage, CNC-derived cells are concentrated (dark blue) at the interface with the epithelium while the peripheral portion of the dental sac is less populated (light blue) with CNC-derived cells. In adulthood, CNC-derived cells contribute to the formation of dentine, pulp and cementum.

derived dental mesenchyme, the size, shape and number of teeth are determined during development. Combinatorial actions of homeobox genes expressed in neural-crest-derived facial mesenchyme have been implicated to specify tooth shape, size and position (Sharpe, 1995; Tucker et al., 1998). Targeted mutation of a number of growth and transcription factor genes resulted in craniofacial malformations including missing teeth, presumably by alteration of migration and differentiation of CNC cells (for review see Thesleff and Sharpe, 1997; Tucker and Sharpe, 1999). To date, the only direct evidence that indicates contribution of CNC cells to tooth and mandibular development during rat embryogenesis was shown by detecting DiI-labeled crest cells from the posterior midbrain in the dental mesenchyme (Imai et al., 1996). But the study only reached bud stage tooth development using a combined in vivo and in vitro approach and showed ectopic labeling in the dental epithelium.

In this study, we have systematically followed the lineage of CNC cells as they contribute to tooth and mandibular morphogenesis. At E11.5 (before the initiation of tooth formation) and E12.5 (when the dental lamina is formed), the CNC-derived ectomesenchyme populates almost the entire region under the oral epithelium (Figs 2F, 3B). As tooth development continues into bud, cap and bell stages, there are increasing numbers of non-CNC-derived cells associated with dental mesenchyme (Figs 3-5). This observation is clearly not due to the fading of labeling of neural crest derivatives, as demonstrated by the strong *lacZ* expression in subsequently formed tooth organs (e.g. 2nd and 3rd molars, data not shown), but results from the possible contribution of non-CNC cells. In parallel, the formation of Meckel's cartilage also shows the highest percentage of CNC-derived ectomesenchymal cells at the initiation site of chondrogenesis and subsequently at the

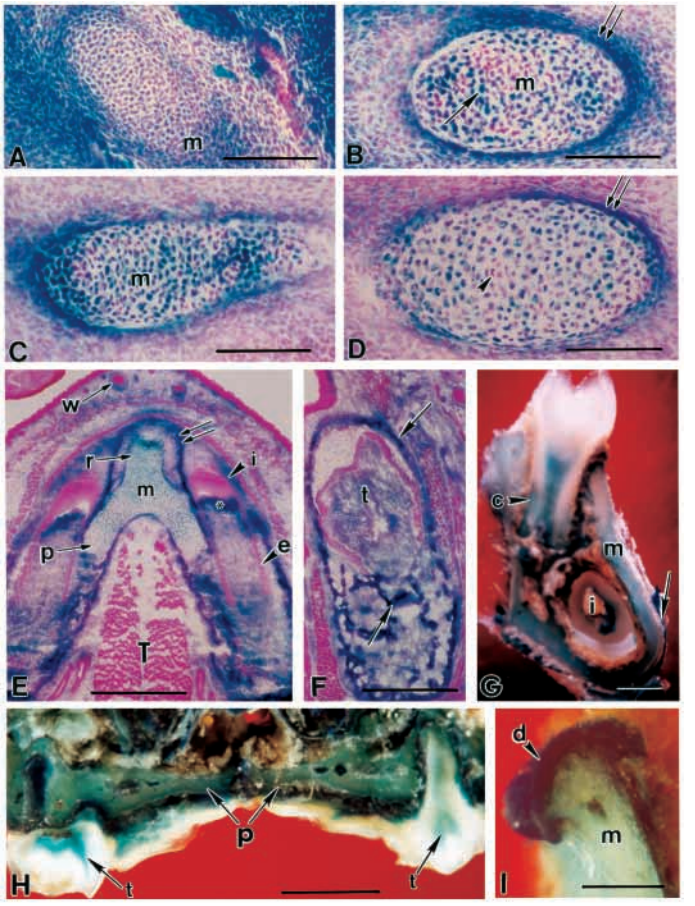

Fig. 6. Contribution of CNC cells during mandibular morphogenesis. (A) At E12.5, CNC-derived ectomesenchyme formed an aggregated cell mass indicating the initiation of Meckel's cartilage (m) formation. (B) At E13.5, CNC-derived cells are mixed with non-CNC-derived cells in Meckel's cartilage. Perichondrium (double arrow) is densely populated with CNC-derived cells. (C) At E14.5, large number of CNC-derived cells is seen in Meckel's cartilage. (D) At E15.5, there is a reduction of CNC-derived cells at the molar region of Meckel's cartilage where chondrogenesis first initiated at E12.5. More non-CNC-derived cells (arrowhead) are present in the cartilage. Double arrow, perichondrium. (E) A transverse section of anterior part of E17.5 mandible shows Meckel's cartilage (m), lower incisor (i), tongue (T) and whisker (W). The anterior (r, rostral) region of Meckel's cartilage is forming and is mainly populated with CNC-derived cells, compared to the posterior end (p) of the cartilage which is formed earlier. The mandible (double arrow) is forming on the lateral side of Meckel's cartilage. The elongated enamel epithelium proliferating zone (e) is a unique feature in rodents, especially for lower incisors. CNC-derived cells are present within incisor dental papilla (*). (F) At birth, molar tooth organ (t) is embedded within the mandible (arrow) populated with CNC-derivatives. (G) In the adult transgenic mouse mandible, the pulp tissue of both incisors (i) and molars, cementum (c), mandible (m) and its periosteum (arrow) show β-gal-positive cells, while enamel tissue of both incisors and molars is not labeled. (H) In a coronal section of adult *Wnt1-Cre/R26R* mouse, *lacZ* expression is present in palatine bone and its periosteum (p), dentine and pulp tissue of maxillary molars (t). (I) The articulating disc (d) of temporomandibular joint (TMJ) receives significant contribution from CNC cells. m, mandibular condyle. Scale bars: A-D, 100 μm; E-G, 0.5 mm; H,I, 1 mm.

chondrogenic front as Meckel's cartilage continues to form by extending both anteriorly and posteriorly (Fig. 6). The dynamic distribution of CNC-derived cells throughout the process of tooth and Meckel's cartilage formation is the most significant finding of this study. This phenomenon might be attributed to apoptosis and/or migration of neural crest cells as well as differential proliferation of neighboring non-CNC-derived cells. Moreover, at least in the formation of Meckel's cartilage in chick embryos, recent studies have identified the ventrally emigrating neural tube (VENT) cells as a significant contributing source in addition to the CNC cells (Sohal et al., 1999). Because there is no *Wnt1* expression in these VENT cells, which will migrate into the first arch after the CNC cells migration, it is tempting to speculate that the non-*lacZ*-expressing cells observed in Meckel's cartilage are derivatives of VENT cells. Alternatively, it is conceivable these *Wnt1*-expressing cells represent only a subpopulation of CNC cells. Based on the observation that progeny of *Wnt1*-expressing cells are found in all predicted CNC-derived structures and there is virtually no ectopic *lacZ* expression, we conclude that *Wnt1-Cre*-mediated *lacZ* expression is an ideal bio-marker to follow at least a significant population of CNC-derived cells during craniofacial development. Additional studies are underway to address some of these critical issues on the fate of CNC-derived cells and to evaluate the stability of the *R26R* reporter gene expression.

Our two-component Cre/lox strategy has clearly demonstrated that all tissues expected to be neural crest origin are labeled with high efficiency, with a virtual absence of ectopic expression, throughout all stages of tooth and skeletal morphogenesis and into adulthood. The results have confirmed all the previous assumptions about the migration and contribution of CNC cells during mammalian embryonic development, which have been largely based on extrapolation from tissue transplantation, short-term labeling and genetic mutations. Moreover, in an accompanying manuscript, the fate of neural crest cells during cardiac development is explored using this two-component Cre/lox strategy (Jiang et al., 2000). Collectively, our studies have provided very comprehensive information on the fate of neural crest cells during the development of mammalian craniofacial structures and cardiac system. Furthermore, this two-component genetic system is not only highly efficient and specific in tracing mouse neural crest derivatives but also can integrate the analysis of the fate and function of mammalian neural crest with mouse molecular genetics in both normal and abnormal embryonic development.

We thank Drs David Crowe, Charles Haun and Harold Slavkin for critical comments on the manuscript. We thank Mal Snead for discussion and encouragement at the beginning of this work. This study was supported by a grant from the NIDCR, NIH (R01 DE12711 to Y. C.). H. M. S was supported by a Grant-in-Aid from the National Center of the American Heart Association, and by a Cardiovascular Research Development Award from the Los Angeles and Western States affiliate of the American Heart Association.

REFERENCES

Anderson, D. J. (1997). Cellular and molecular biology of neural crest cell lineage determination. *Trends Genet.* **13,** 276-280.

Artinger, K. B., Chitnis, A. B., Mercola, M., and Driever, W. (1999). Zebrafish narrowminded suggests a genetic link between formation of neural crest and primary sensory neurons. *Development* **126**, 3969-3979.

Bronner-Fraser, M. (1993). Mechanisms of neural crest migration. *BioEssays* **15**, 221-230.

Bronner-Fraser, M. (1995). Origins and developmental potential of the neural crest. *Exp. Cell Res.* **2,** 405-417.

Chai, Y., Mah, A., Crohin, C., Groff, S., Bringas, P., Le, T., Santos, V. and Slavkin, H. C. (1994) Specific transforming growth factor-beta subtypes regulate embryonic mouse Meckel's cartilage and tooth development. *Dev. Biol*. **162,** 85-103.

Chai, Y., Sasano, Y., Bringas, P., Mayo, M., Kaartinen, V., Heisterkamp, N., Groffen, J., Slavkin, H. C., and Shuler, C. (1997) Characterization of the fate of midline epithelial cells during the fusion of mandibular prominences in vivo. *Dev. Dyn*. **208,** 526-535.

Chai, Y., Bringas, P. Jr., Shuler, C., Devaney, E., Grosschedl, R. and Slavkin, H. C. (1998). A mouse mandibular culture model permits the study of neural crest cell migration and tooth development. *Int. J. Dev. Biol.* **42,** 87-94.

Chan, W. Y. and Tam, P. P. L. (1988). A morphological and experimental study of the mesencephalic neural crest cells in the mouse embryo using wheat germ agglutinin-gold conjugate as the cell marker. *Development* **102,** 427-442.

Danielian, P. S., Muccino, D., Rowitch, D. H., Michael, S. K. and McMahon, A. P. (1998). Modification of gene activity in mouse embryos in utero by a tamoxifen-inducible form of Cre recombinase. *Curr. Biol.* **8**, 1323-1326.

Dorsky, R. I., Moon, R. T. and Raible, D. W. (1998). Control of neural crest cell fate by the Wnt signaling pathway. *Nature* **396**, 370-373.

Echelard, Y., Vassileva, G. and McMahon, A. P. (1994). *Cis*-acting regulatory sequences governing *Wnt*-1 expression in the developing mouse CNS. *Development* **120**, 2213-2224.

Friedrich, G. and Soriano, P. (1991). Promoter traps in embryonic stem cells: a genetic screen to identify and mutate developmental genes in mice. *Genes Dev.* **5,** 1513-1523.

Graham, A. and Lumsden, A. (1993) The role of segmentation in the development of the branchial region of higher vertebrate embryos. In *Blastogenesis, Normal and Abnormal* (ed. J. M. Opitz), pp. 99-108, New York: Wiley-Liss Publishers.

Herbarth, B., Pingaulk, V., Bondurand, N., Kuhlbrodt, K., Hermans-Borgmeyer, I., Puliti, A., Lemort, N., Goossens, M. and Wegner, M. (1998). Mutation of the Sry-related Sox10 gene in Dominant megacolon, a mouse model for human Hirschsprung disease. *Proc. Natl. Acad. Sci. USA* **95**, 5161-5165.

Ikeya, M., Lee, S. M., Johnson, J. E., McMahon, A. P. and Takada, S. (1997). Wnt signaling required for expansion of neural crest and CNS progenitors. *Nature* **389**, 966-970.

Imai, H., Osumi-Yamashita, N., Ninomiya, Y. and Kazuhiro, E. (1996). Contribution of early-emigrating midbrain crest cells to the dental mesenchyme of mandibular molar teeth in rat embryos. *Dev. Biol.* **176,** 151-165.

Jiang, X., Rowitch, D. H., Soriano, P., McMahon, A. P. and Sucov, H. M. (2000). Fate of the mammalian cardiac neural crest. *Development* **127**, 1607-1616.

Koch, W. E. (1967). In vitro differentiation of tooth rudiments of embryonic mice. I. Transfilter interaction of embryonic incisor tissues. *J. Exp. Zool.* **165,** 155-170.

Kollar, E. J. and Baird, G. (1969). The influence of the dental papilla on the development of tooth shape in embryonic mouse tooth germs. *J. Embryol. Exp. Morph.* **21**, 131-148.

Kollar, E. J. and Lumsden, A. G. S. (1979). Tooth morphogenesis: The role of the innervation during induction and pattern formation. *J. Biol. Buccale* **7,** 49-60.

LaBonne, C. and Bronner-Fraser, M. (1999). Molecular mechanisms of neural crest formation. *Annu. Rev. Cell Dev. Biol.* **15,** 81-112.

Le Douarin, N., Ziller, C. and Coul, G. (1993). Patterning of neural crest derivatives in the avian embryo: In vivo and in vitro studies. *Dev. Biol.* **159,** 24-49.

Lumsden, A. G. S. (1988). Spatial organization of the epithelium and the role of neural crest cells in the initiation of the mammalian tooth. *Development* **103 Supplement**, 55-169.

Lumsden, A. and Krumlauf, R. (1996). Patterning the vertebrate neuraxis. *Science* **274**, 1109-1115.

McMahon, A. P., Joyner, A. L., Bradley, A. and McMahon, J. A. (1992). The midbrain-hindbrain phenotype of *Wnt-1*$^{-}$/*Wnt-1*$^{-}$ mice results from

stepwise deletion of *engrailed*-expressing cells by 9.5 days post-coitum. *Cell* **69**, 581-595.

McMahon, A. P. and Bradley, A. (1990). The *Wnt*-(*int*-1) proto-oncogene is required for development of a large region of the mouse brain. *Cell* **62,** 1073-1985.

Mina, M. and Kollar, E. J. (1987). The induction of odontogenesis in non-dental mesenchyme combined with early murine mandibular arch epithelium. *Arch. Oral Biol.* **32,** 123-127.

Nichols, D. H. (1981). Neural crest formation in the head of the mouse embryo as observed using a new histological technique. *J. Embryol Exp. Morph.* **64,** 105-120.

Noden, D. M. (1983). The role of the neural crest in patterning of avian cranial skeletal, connective, and muscle tissue. *Dev. Biol.* **96,** 144-165.

Noden, D. M. (1991). Cell movements and control of patterned tissue assembly during craniofacial development. *J. Craniofac. Genet. Dev. Biol.* **11**, 192-213.

Osumi-Yamashita, N., Noji, S., Nohno, T., Koyama, E., Doi, H., Eto, K. and Taniguchi, S. (1990) Expression of retinoic acid receptor genes in neural crest-derived cells during mouse facial development. *FEBS Lett.* **264,** 71-74.

Osumi-Yamashita, Ninomiya, Y., Doi, H. and Eto, K. (1994). The contribution of both forebrain and midbrain crest cells to the mesenchyme in the frontonasal mass of mouse embryos. *Dev. Biol.* **164**, 409-419.

Poelmann, R. E. and Gittenberger-de Groot, A. C. (1999). A subpopulation of apoptosis-prone cardiac neural crest cells targets to the venous pole: multiple functions in heart development? *Dev. Biol.* **207**, 271-286.

Romer, A. S. (1972). The vertebrate as a dual animal-somatic and visceral. *Evolutionary Biology* **6,** 121-156.

Saldivar, J. R., Sechrist, J. W., Krull, C. E., Ruffins, S. and Bronner-Fraser, M. (1997). Dorsal hindbrain ablation results in rerouting of neural crest migration and changes in gene expression, but normal hyoid development. *Development* **14,** 2729-2739.

Selleck, M. A. J., Scherson, T. Y. and Bronner-Fraser, M. (1993). Origins of neural crest cell diversity. *Dev. Biol.* **159**, 1-11.

Serbedzija, G. N., Bronner-Fraser, M. and Fraser, S. E. (1989). A vital dye analysis of the timing and pathways of avian trunk neural crest cell migration. *Development* **106**, 809-816.

Serbedzija, G. N., Bronner-Fraser, M. and Fraser, S. E. (1992) Vital dye analysis of cranial neural crest cell migration in the mouse embryo. *Development*, **116**: 297-307.

Sharpe, P. T. (1995). Homeobox genes and orofacial development. *Connect. Tissue Res.* **32,** 17-25.

Smith, M. M. and Hall, B. K. (1993). A developmental model for evolution of the vertebrate exoskeleton and teeth: the role of cranial and trunk neural crest. *Evol. Biol.* **27,** 387-448.

Sohal, G. S., Ali A. A. and Dai, D. (1999). Ventrally emigrating neural tube cells contribute to the formation of Meckel's and quadrate cartilage. *Dev. Dyn.* **216,** 37-44.

Soriano, P. (1999). Generalized *lac*Z expression with the ROSA26 Cre reporter strain. *Nature Genetics* **21,** 70-71.

Tan, S. S. and Morriss-kay, G. M. (1986). The development and distribution of the cranial neural crest in the rat embryo. *Cell Tiss. Res.* **240,** 403-416.

Theiler, K. (1989). *The House Mouse*. Amsterdam: Springer-Verlag.

Thesleff, I. and Sharpe, P. (1997). Signaling networks regulating dental development. *Mech. Dev.* **67,** 111-123.

Thomas, K. R., Musci, T. S., Neumann, P. E. and Capecchi, M. R. (1991). *Swaying* is a mutant allele of the proto-oncogene *Wnt*-1. *Cell* **67,** 969-976.

Thomas, K. R. and Capeechi, M. R. (1990). Targeted disruption of the murine *int*-1 proto-oncogene resulting in severe abnormalities in midbrain and cerebellar development. *Nature* **346,** 847-850.

Trumpp, A., Depew, M. J., Rubenstein, J. L. R., Bishop, J. M. and Martin, G. R. (1999). Cre-mediated gene inactivation demonstrates that FGF8 is required for cell survival and patterning of the first branchial arch. *Genes Dev.* **13**, 3136-3148.

Tucker, A. S., Matthews, K. L. and Sharpe, P. T. (1998). Transformation of tooth type induced by inhibition of BMP signaling. *Science* **282**, 1136-1138.

Tucker, A. S. and Sharpe, P. T. (1999). Molecular genetics of tooth morphogenesis and pattering: the right shape in the right place. *J. Dent. Res.* **78,** 826-834.

Tucker, G. C., Aoyama, H., Lipinski, M., Tursz, T. and Thiery, J. P. (1984). Identical reactivity of monoclonal antibodies HNK-1 and NC-1: conservation in vertebrates on cells derived from the neural primordium and on some leukocytes. *Cell Differ*. **14**, 223-230.

Wilkinson, D. G. Bailes, J. A., Champion, J. F., and McMahon, A. P. (1987). Expression of the proto-oncogene int-1 is restricted to specific neural cells in the developing mouse embryo. *Cell* **50**, 79-88.

Woo, K., and Fraser, S. E. (1998). Specification of the hindbrain fate in the zebrafish. *Dev. Biol*. **197**, 283-296.

Yamauchi, Y., Abe, K., Mantani, A., Hitoshi, Y., Suzuki, M., Osuzu, F., Kuratani, S. and Yamamura, K. (1999). A novel transgenic technique that allows specific marking of the neural crest cell lineage in mice. *Dev. Biol.* **212,** 191-203.

Zambrowicz, B. P., Imamoto, A., Fiering, S., Herzenberg, L. A., Kerr, W. G. and Soriano, P. (1997). Disruption of overlapping transcripts in the ROSA βgeo 26 gene trap strain leads to widespread expression of β-galactosidase in mouse embryos and hematopoietic cells. *Proc. Natl. Acad. Sci. USA* **94,** 3789-3794.